

Crystal structures of $\text{CaNiSi}_2\text{O}_6$ and $\text{CaCoSi}_2\text{O}_6$ and some crystal-chemical relations in $C2/c$ clinopyroxenes

SUBRATA GHOSE, CH'ENG WAN, FUJIO P. OKAMURA*

Department of Geological Sciences, University of Washington, Seattle, Washington 98195, U.S.A.

ABSTRACT

Synthetic clinopyroxenes $\text{CaNiSi}_2\text{O}_6$ and $\text{CaCoSi}_2\text{O}_6$ are monoclinic, space group $C2/c$ with unit-cell dimensions $a = 9.734(2)$, $b = 8.891(2)$, $c = 5.228(1)$ Å, $\beta = 105.87(2)^\circ$ and $a = 9.806(1)$, $b = 8.950(1)$, $c = 5.243(1)$ Å, $\beta = 105.45(1)^\circ$, respectively. Their crystal structures have been refined by the method of least squares based on 1152 and 984 reflections measured on an automated single-crystal X-ray diffractometer to R factors of 0.047 and 0.025. The average octahedral Ni–O and Co–O bond lengths are 2.070 and 2.101 Å, whereas the corresponding average Ca–O distances are 2.894 and 2.930 Å. Although the average Si–O bond lengths are nearly identical (1.637 and 1.636 Å), significant differences in individual Si–O bond lengths exist in the two compounds. The stereochemical relations in the four series of stoichiometric $C2/c$ pyroxenes $\text{CaM}^{2+}\text{Si}_2\text{O}_6$, $\text{CaM}^{3+}\text{AlSiO}_6$, $\text{NaM}^{3+}\text{Si}_2\text{O}_6$, and $\text{LiM}^{3+}\text{Si}_2\text{O}_6$ can be explained on the basis of steric effect, whereby the absolute shapes and sizes of the constituent polyhedra in the clinopyroxene structure depend on their interaction with adjacent polyhedra. The average Si–O_{br} bond length, the tetrahedral edge [O(3)–O(3')] and the chain-kinking angle [O(3)–O(3')–O(3'')] within each series depend on the ratio of the $\langle\text{M}(1)\text{--O}\rangle$ and $\langle\text{M}(2)\text{--O}\rangle$ bond lengths.

INTRODUCTION

Crystal chemistry of transition-metal-bearing pyroxenes is of interest from the point of view of providing a fundamental understanding of the relationships among crystal structures, chemical bonding, thermodynamic and magnetic properties, and stability relations. Such details are also valuable in understanding the partitioning of the transition-metal ions among coexisting orthopyroxenes, clinopyroxenes, and olivines in mafic and ultramafic rocks and their bearing on petrogenesis. In 1975, we determined the crystal structures of synthetic clinopyroxenes $\text{CaNiSi}_2\text{O}_6$ and $\text{CaCoSi}_2\text{O}_6$ and derived some crystal-chemical relationships among stoichiometric clinopyroxenes with $C2/c$ symmetry (Ghose and Wan, 1975). These structures were determined independently by Schlenker (1976) as a part of a Ph.D. dissertation at Virginia Polytechnic Institute and State University, Blacksburg, Virginia. Although some of the details of these structures have appeared in discussions of crystal-chemical relations of pyroxenes (Ribbe and Prunier, 1977; Cameron and Papike, 1980, 1981), complete structural details have not yet been published. In view of their importance in understanding the crystal-chemical behavior of $C2/c$ clinopyroxenes, we decided to publish our results, which are slightly more precise than Schlenker's. We also offer some crystal-chemical insights complementary to those

already provided by Clark et al. (1969), Ribbe and Prunier (1977), and Cameron and Papike (1980, 1981).

EXPERIMENTAL DETAILS

Synthesis

Both samples of $\text{CaNiSi}_2\text{O}_6$ and $\text{CaCoSi}_2\text{O}_6$ were synthesized for calorimetric measurements by Navrotsky and Coons (1976). $\text{CaNiSi}_2\text{O}_6$ was prepared by crystallizing a melt formed by holding a mix of NiO, CaCO₃, and SiO₂ above the melting point of the pyroxene (1340°C). $\text{CaCoSi}_2\text{O}_6$ was prepared from CaCO₃, Co₃O₄ and SiO₂ at 1460°C by a sintering technique. Portions were obtained for the structure determination through the courtesy of A. Navrotsky.

TABLE 1. $\text{CaNiSi}_2\text{O}_6$ and $\text{CaCoSi}_2\text{O}_6$: Crystal data

	$\text{CaNiSi}_2\text{O}_6$		$\text{CaCoSi}_2\text{O}_6$	
	Ghose and Wan (1975)	Schlenker (1976)	Ghose and Wan (1975)	Schlenker (1976)
a (Å)	9.734(2)	9.737(2)	9.806(1)	9.797(1)
b (Å)	8.891(2)	8.899(2)	8.950(1)	8.954(1)
c (Å)	5.228(1)	5.231(1)	5.243(1)	5.243(1)
β (°)	105.87(2)	105.92(1)	105.45(1)	105.40(2)
V (Å ³)	435.21(16)	435.88	443.51(10)	443.43
d_c (g/cm ³)	3.831	3.825	3.764	3.761
No. of reflections	1152	1173	984	627
R	0.047	0.077	0.025	0.051
R_w	0.041	0.071	0.030	0.052

* Present address: National Institute for Researches in Inorganic Materials, Kurakake, Sakura-mura, Niihari-gun Ibaraki 300-31, Japan.

TABLE 2a. Clinopyroxenes CaNiSi₂O₆ and CaCoSi₂O₆: Atomic positional and equivalent isotropic thermal parameters

Atom site	Occu-pancy	x	y	z	B _{eq}
CaNiSi ₂ O ₆					
M(1)	Ni	0	0.90911(6)	0.25	0.34(1)
M(2)	Ca	0	0.29816(1)	0.25	0.59(1)
T	Si	0.28733(8)	0.09298(9)	0.22752(14)	0.33(1)
O(1)		0.1153(2)	0.0861(2)	0.1414(4)	0.50(3)
O(2)		0.3603(2)	0.2508(2)	0.3188(4)	0.59(3)
O(3)		0.3514(2)	0.0191(2)	-0.0081(4)	0.51(3)
CaCoSi ₂ O ₆					
M(1)	Co	0	0.90750(3)	0.25	0.46(1)
M(2)	Ca	0	0.29907(5)	0.25	0.72(1)
T	Si	0.28727(5)	0.09262(5)	0.23080(9)	0.41(1)
O(1)		0.1176(1)	0.0881(1)	0.1473(2)	0.58(2)
O(2)		0.3613(1)	0.2487(1)	0.3222(2)	0.74(2)
O(3)		0.3508(1)	0.0192(1)	-0.0061(2)	0.61(2)

Note: Standard deviations in parentheses.

Determination of unit-cell dimensions and collection of X-ray intensity data

The unit-cell dimensions (Table 1) were determined by least-squares refinement of 2θ values of 15 reflections measured with monochromatized MoK α radiation on a Syntex P1 single-crystal diffractometer. The monochromatization was achieved by reflection from a graphite "single" crystal. Our unit-cell dimensions are in good agreement with those measured by Schlenker (1976). The X-ray intensity data were collected on the same crystals used for unit-cell measurements by the $\theta/2\theta$ scan method using monochromatized MoK α radiation and a variable scan rate. Because of the small sizes of the crystals (CaNiSi₂O₆: 0.04 × 0.06 × 0.08 mm; CaCoSi₂O₆: 0.06 × 0.08 × 0.12 mm), the minimum scan rate was 0.5°/min. (50 kV, 12 mA). All reflections within a 2θ limit of 70° and 65° for CaNiSi₂O₆ and CaCoSi₂O₆, respectively, were measured and subsequently corrected for Lorentz and polarization factors. Absorption corrections were neglected because of small crystal sizes.

TABLE 2b. CaNiSi₂O₆ and CaCoSi₂O₆: Anisotropic thermal parameters

Atom	β_{11}	β_{22}	β_{33}	β_{12}	β_{13}	β_{23}
CaNiSi ₂ O ₆						
Ni	103(5)	115(5)	314(16)	0	72(6)	0
Ca	196(8)	185(8)	438(26)	0	28(11)	0
Si	95(7)	110(8)	343(22)	6(7)	88(9)	-1(12)
O(1)	138(18)	175(20)	490(59)	4(17)	113(26)	9(32)
O(2)	199(21)	147(20)	562(67)	-21(17)	75(29)	-5(32)
O(3)	145(18)	194(20)	442(62)	7(18)	112(27)	-73(31)
CaCoSi ₂ O ₆						
Co	136(3)	142(3)	415(10)	0	45(4)	0
Ca	227(5)	210(5)	551(15)	0	0(6)	0
Si	113(4)	129(5)	398(14)	-7(3)	57(6)	-9(6)
O(1)	128(10)	209(12)	580(36)	1(9)	70(15)	17(17)
O(2)	255(12)	161(12)	768(40)	-65(10)	105(18)	-26(18)
O(3)	156(11)	226(12)	538(37)	-3(9)	90(16)	-116(17)

Note: Standard deviations in parentheses (× 10⁵).

TABLE 3a. CaNiSi₂O₆: Dimensions and orientations of thermal-vibration ellipsoids

Atom	Axis	RMS amplitude (Å)	Angle (°) with a	Angle (°) with b	Angle (°) with c
M(1) (Ni)	1	0.059	61(11)	90	45(11)
	2	0.068	90	180	90
	3	0.069	165(79)	90	59(79)
M(2) (Ca)	1	0.074	104(6)	90	2(6)
	2	0.086	90	180	90
	3	0.098	142(6)	90	112(6)
Si	1	0.055	51(13)	83(10)	55(13)
	2	0.067	88(17)	165(23)	76(18)
	3	0.071	139(36)	77(35)	37(37)
O(1)	1	0.069	52(27)	90(15)	54(27)
	2	0.082	65(138)	37(77)	112(130)
	3	0.085	117(128)	37(108)	65(145)
O(2)	1	0.075	105(19)	15(20)	88(25)
	2	0.085	87(21)	83(26)	165(20)
	3	0.097	145(18)	102(13)	107(18)
O(3)	1	0.062	63(14)	71(10)	48(11)
	2	0.082	16(41)	105(38)	109(38)
	3	0.093	93(19)	29(17)	117(11)

Refinement of the crystal structures

The crystal structures were refined by the method of least-squares by the program RFINE (Finger, 1969). The atomic positional parameters of diopside, CaMgSi₂O₆ (Clark et al., 1969), were used as input parameters. The atomic scattering factors of Ca, Ni, Co, Si, and O used for the structure-factor calculations were taken from Cromer and Waber (1965) and were corrected for anomalous dispersion (Cromer, 1965). The structure factors (F_o values) were weighted as $F_o/\sigma^2(F_o)$, where $\sigma(F_o)$ is the standard deviation of measurement as determined from counting statistics. In both cases, three cycles of refinement using isotropic temperature factors, followed by three more cycles using anisotropic ones, led to conver-

TABLE 3b. CaCoSi₂O₆: Dimensions and orientations of atomic thermal-vibration ellipsoids

Atom	Axis	RMS amplitude (Å)	Angle (°) with a	Angle (°) with b	Angle (°) with c
M(1) (Co)	1	0.075	111(12)	90	5(12)
	2	0.076	90	180	90
	3	0.081	139(9)	90	115(9)
M(2) (Ca)	1	0.080	116(5)	90	10(5)
	2	0.092	90	180	90
	3	0.111	137(2)	90	118(2)
Si	1	0.070	134(71)	44(71)	75(83)
	2	0.071	119(37)	94(27)	135(37)
	3	0.074	121(43)	146(48)	69(54)
O(1)	1	0.076	160(12)	91(8)	95(12)
	2	0.086	99(14)	72(18)	149(17)
	3	0.093	87(8)	21(19)	71(20)
O(2)	1	0.073	113(6)	24(6)	89(5)
	2	0.100	95(8)	85(5)	159(8)
	3	0.114	147(8)	111(7)	100(8)
O(3)	1	0.071	74(10)	62(5)	43(7)
	2	0.084	15(8)	97(8)	92(10)
	3	0.105	86(6)	145(9)	58(7)

TABLE 6. Selected interatomic distances and angles in *C2/c* clinopyroxenes

	Avg. M(1)–O (Å)	Avg. M(2)–O (Å)	Avg. T–O _{br} (Å)	Avg. T–O _{nbr} (Å)	O(3)–O(3') (Å)	O(3)–O(3')–O(3'') (°)	Ref.*
CaNiSi ₂ O ₆	2.070	2.496	1.672	1.601	2.639(1)	165.2(2)	1
CaMgSi ₂ O ₆	2.077	2.498	1.676	1.594	2.644(3)	166.4(1)	2
CaCoSi ₂ O ₆	2.101	2.502	1.675	1.597	2.644(1)	165.1(1)	1
CaFeSi ₂ O ₆	2.130	2.511	1.676	1.593	2.647(1)	164.5(1)	3
CaMnSi ₂ O ₆	2.173	2.450	1.688	1.599	2.673(3)	163.8(5)	4
CaAlAlSiO ₆	1.947	2.461	1.692	1.679	2.657(2)	165.9(1)	5
CaFe ³⁺ AlSiO ₆	2.024	2.484	1.713	1.683	2.709(2)	164.4(1)	6
CaSc ³⁺ AlSiO ₆	2.102	2.513	1.714	1.677	2.749(1)	164.2(1)	7
NaAlSi ₂ O ₆	1.929	2.469	1.634	1.616	2.614(1)	174.6(1)	2
NaFeSi ₂ O ₆	2.025	2.518	1.642	1.614	2.651(1)	174.0(2)	2
NaCr ³⁺ Si ₂ O ₆	1.998	2.489	1.643	1.606	2.643(5)	172.1(2)	2
NaSc ³⁺ Si ₂ O ₆	2.102	2.564	1.653	1.611	2.681(1)	173.6(1)	8
NaN ³⁺ Si ₂ O ₆	2.141	2.568	1.652	1.612	2.688(1)	170.8(2)	9
LiAlSi ₂ O ₆	1.919	2.211	1.624	1.612	2.616(1)	170.5(2)	2
LiFe ³⁺ Si ₂ O ₆	2.031	2.249	1.626	1.612	2.647(1)	180.0(2)	2
LiSc ³⁺ Si ₂ O ₆	2.107	2.289	1.630	1.618	2.678(1)	175.6(1)	10

Site occupancies

CaAlAlSiO₆: M(2): Ca; M(1): Al, T: Al 0.5, Si 0.5CaFeAlSiO₆: M(2): Ca; M(1): Fe 0.821, Al 0.179; T: Si 0.5, Al 0.411, Fe 0.089CaSc³⁺AlSiO₆: M(2): Ca; M(1): Sc³⁺, T: Al³⁺ 0.5, Si⁴⁺ 0.5

* References: (1) This paper; (2) Clark et al. (1969); (3) Cameron et al. (1973); (4) Freed and Peacor (1967); (5) Okamura et al. (1973); (6) Ghose et al. (1986); (7) Ohashi and Ii (1978); (8) Hawthorne and Grundy (1973); (9) Hawthorne and Grundy (1974); (10) Hawthorne and Grundy (1977).

RESULTS

Unit-cell dimensions

In the series of CaM²⁺Si₂O₆ pyroxenes where M²⁺ = Ni²⁺, Mg²⁺, Fe²⁺, Co²⁺, and Mn²⁺, the unit-cell dimensions and volumes are expected to be linear functions of the M²⁺ cation radius. However, significant negative deviations from linearity, particularly in unit-cell dimensions *a* and *b* and the unit-cell volume *V* (Fig. 1), are observed. These results are at variance with linear relationships derived by Ribbe and Prunier (1977) for a larger set of *C2/c* type pyroxenes.

On the basis of the observed ⟨M(1)–O⟩ distances in CaM²⁺Si₂O₆ pyroxenes, where M²⁺ = Ni²⁺, Mg²⁺, Co²⁺, Fe²⁺, and Mn²⁺ (Table 6), we can calculate the effective ionic radius of the M(1) cation, assuming the oxygen ionic radius to be 1.40 Å. These radii in ångstroms are shown in Table 7 along with those of Shannon and Prewitt (1970).

The M(1) cation radii in clinopyroxenes are systematically smaller than the Shannon-Prewitt radii, which were derived from oxides and fluorides. Similar discrepancies are also observed for the series NaM³⁺Si₂O₆ and

LiM³⁺Si₂O₆, where M³⁺ = Al³⁺, Fe³⁺, Cr³⁺, Sc³⁺, and In³⁺. This fact indicates that the M(1)–O bonding in clinopyroxenes is more covalent than that in corresponding oxides. A plot of the unit-cell dimensions vs. the effective ionic radii in clinopyroxenes yields nearly linear relation-

TABLE 7. Effective ionic radius (in Å) of the M(1) cation

	Cpx	Shannon and Prewitt (1970)	Δ
Ni ²⁺	0.670	0.69	0.02
Mg ²⁺	0.677	0.72	0.043
Co ²⁺	0.701	0.745	0.044
Fe ²⁺	0.730	0.78	0.050
Mn ²⁺	0.773	0.83	0.057

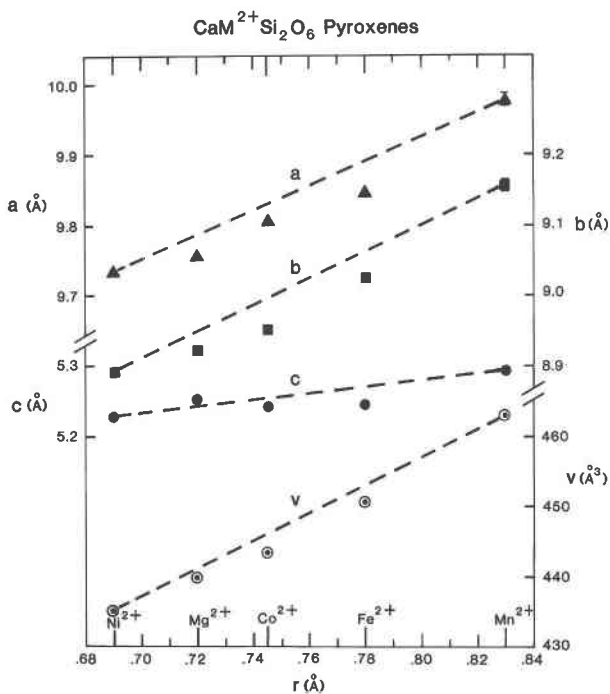


Fig. 1. Unit-cell dimensions and volume of CaM²⁺Si₂O₆ pyroxenes as a function of the M(1) cation radius. Ionic radii values from Shannon and Prewitt (1970).

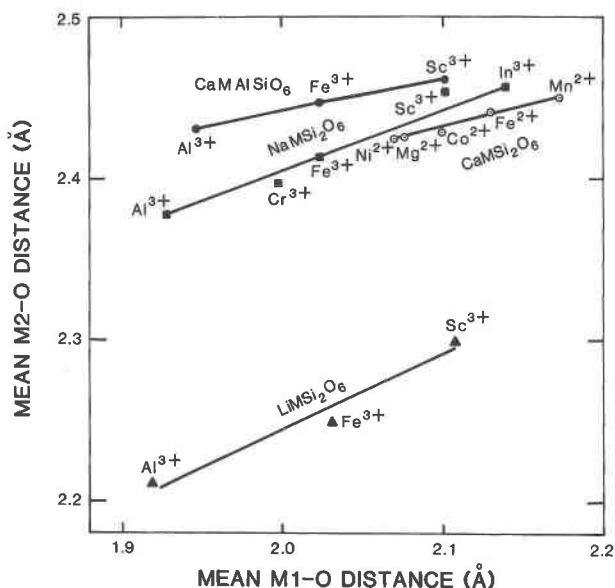


Fig. 2. Mean M(2)-O vs. mean M(1)-O bond lengths in $C2/c$ pyroxenes.

ships. Hence, these radii may be more useful in exploring structural effects of cation substitution in pyroxenes.

The M(1) octahedron

As expected, the Ni octahedron (avg. Ni-O bond length 2.070 Å) is considerably smaller than the Co octahedron (avg. Co-O bond length 2.101 Å). Both octahedra are

very nearly regular, although the Co octahedron appears to be slightly more distorted than the Ni octahedron as evidenced from the difference of the shortest and the longest M-O bond distances ($\Delta \text{Co-O}$: 0.065 Å; $\Delta \text{Ni-O}$: 0.051 Å). The average angular deviations from an ideal octahedral angle are similar in both cases (avg. $\Delta \text{O-M-O}$: Co 3.20°; Ni 3.45°).

The M(2) polyhedron

Although very similar in size and shape, the Ca polyhedron in $\text{CaCoSi}_2\text{O}_6$ ($\langle \text{Ca-O} \rangle = 2.930$ Å) is slightly larger than that in $\text{CaNiSi}_2\text{O}_6$ ($\langle \text{Ca-O} \rangle = 2.894$ Å). This result can be explained by the observation made by Okamura et al. (1974) that the size of the Ca polyhedron in a clinopyroxene depends on the occupancy and size of the M(1) octahedron. Within the two Ca polyhedra, the M(2)-O(1) and M(2)-O(2) distances are nearly identical, whereas the M(2)-O(3) distances show significant differences. This is consistent with the fact that the O(3) oxygen is considerably overbonded (2.5 e.v.u.), whereas O(1) and O(2) are underbonded (O(1), 1.92; O(2), 1.58 e.v.u.). Hence, the M(2)-O(3) bonds are more flexible for the purposes of structural adjustments than M(2)-O(1) and M(2)-O(2) bonds. These bonds are also affected most during thermal expansion (Cameron et al., 1973) and compression (Levien and Prewitt, 1981).

The Si tetrahedron

The particular bonding characteristics of the oxygen atoms manifest themselves in determining the individual

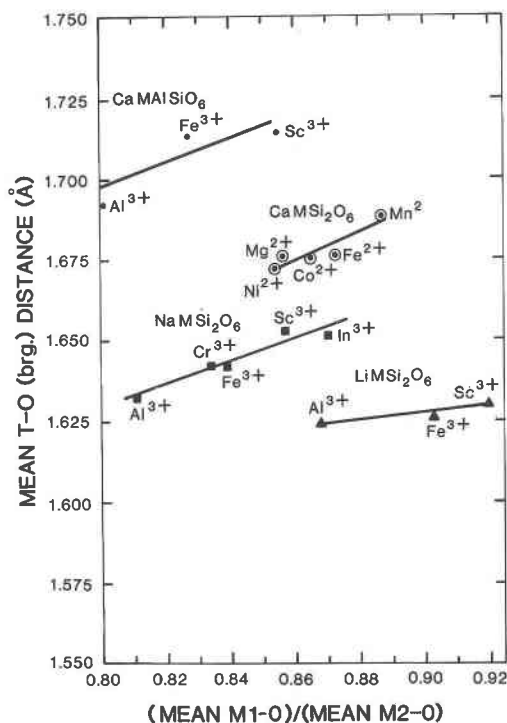
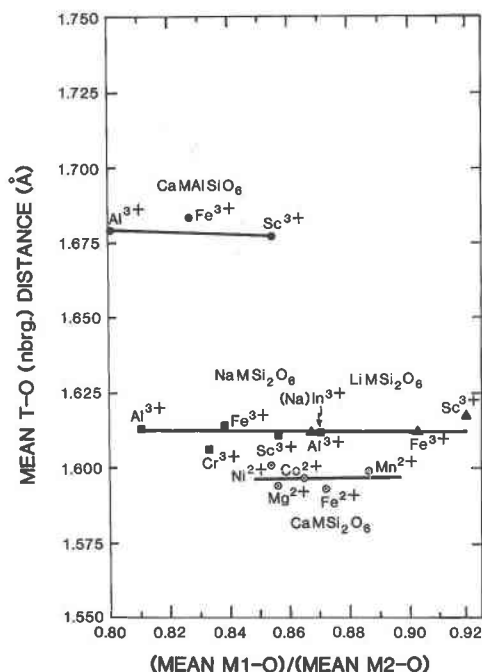


Fig. 3. Mean Si-O_{nbr} (left) and Si-O_{br} (right) bond lengths as a function of the ratio of mean M(2)-O and mean M(1)-O bond lengths in $C2/c$ pyroxenes.

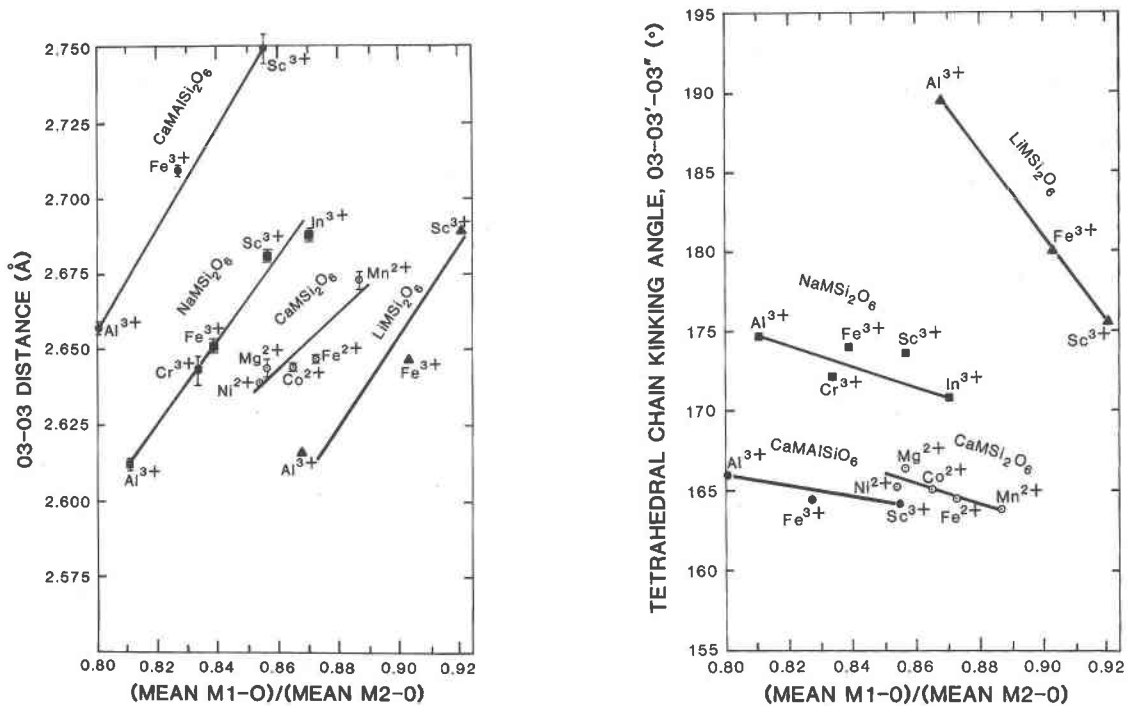


Fig. 4. The silicate tetrahedral edge distance O(3)-O(3') (left) and the silicate-chain kinking angle O(3)-O(3')-O(3'') (right) as a function of the ratio $\langle M(2)-O \rangle$ and $\langle M(1)-O \rangle$ bond lengths in *C2/c* pyroxenes. The straight lines through the points are intended as guides and do not necessarily imply linear fits.

Si-O bond lengths (Clark et al., 1969; Ribbe and Prunier, 1977). The nonbridging Si-O(2) bond lengths (1.588 Å) in both structures are the shortest and are nearly identical to those in other CaM²⁺Si₂O₆ pyroxenes. This is due to the severe underbonding of O(2). The Si-O(1) bond length in CaNiSi₂O₆ (1.614 Å) is somewhat larger than that in CaCoSi₂O₆ (1.605 Å), as observed also by Schlenker (1976), whose respective values are 1.606 and 1.599 Å. This difference can be explained by the fact that the O(1) oxygens are much more closely bonded to Ni [avg. Ni-O(1), 2.076 Å] than to Co [avg. Co-O(1), 2.116 Å]. The slightly larger avg. Si-O(3)_{br} bond length and the O(3)-O(3') edge distance in CaCoSi₂O₆ compared to those in CaNiSi₂O₆ may be significant in view of the steric effects discussed below. The silicate-chain kinking angles are nearly identical in both structures [Ni, 165.2(2)°; Co, 165.1(1)°].

CRYSTAL-CHEMICAL RELATIONS IN *C2/c* CLINOPYROXENES

Crystal-chemical relations in *C2/c* clinopyroxenes have been previously discussed in terms of (1) ionic radii of cations occupying the M(1) and M(2) sites, (2) Pauling bond strengths received by the oxygen atoms, and (3) electronegativity differences (Clark et al., 1969; Ribbe and Prunier, 1977; Hawthorne and Grundy, 1977; Cameron and Papike, 1980, 1981). We would like to draw attention to another factor, namely, "the steric effect," which is important in determining the absolute shapes and sizes

of the constituent polyhedra in a clinopyroxene structure. Ghose and Wan (1975) recognized four distinct series of *C2/c* clinopyroxenes: CaM²⁺Si₂O₆, CaM³⁺AlSiO₆, NaM³⁺Si₂O₆, and LiM³⁺Si₂O₆, within each of which the absolute size of the M(2) polyhedron depends on the size of the adjacent M(1) octahedron; furthermore, the Si-O_{br} and O(3)-O(3') tetrahedral edge distances and the tetrahedral-chain kinking angles [O(3)-O(3')-O(3'')] depend on the ratio of the $\langle M(1)-O \rangle$ and $\langle M(2)-O \rangle$ distances. The size of the M(1) octahedron also depends on the size of the M(2) polyhedron. For example, the average M(1)(Al)-O distances in spodumene (LiAlSi₂O₆), jadeite (NaAlSi₂O₆), and Tschermak's pyroxene (CaAlAlSi₂O₆) are 1.919, 1.928, and 1.947 Å, respectively (Clark et al., 1969; Okamura et al., 1974). From a rigid-group thermal-vibration analysis of the enstatite structure from neutron-diffraction data, Ghose et al. (1987) concluded that the SiO₄ tetrahedron is the most rigid and the M(2) octahedron is the least-rigid polyhedron; even so, within the SiO₄ tetrahedron the O(3)-O(3') edge is quite flexible. The above results can be summarized in terms of a theorem:

Within the pyroxene structure, all polyhedra (including SiO₄ tetrahedra) are inherently flexible, and their absolute shapes and sizes are dependent on the interaction with the adjacent polyhedra.

This effect is also applicable to other nearly close-packed structures, such as olivines and garnets. We may call it the "steric effect," which is a secondary effect, whereas

the effects due to ionic radii and Pauling bond strengths are primary ones. All three effects are important in determining the steric details of the pyroxene structure. The effect due to electronegativity differences, not yet been fully explored, is most likely a secondary effect. It is the neglect of the steric effect that forced Ribbe and Prunier (1977) to postulate the variable charge q on the M(2) cation. In Figure 2, we show the interdependence of the $\langle\text{M}(1)\text{-O}\rangle$ and $\langle\text{M}(2)\text{-O}\rangle$ distances in the four series of pyroxenes, $\text{CaM}^{2+}\text{Si}_2\text{O}_6$, $\text{CaM}^{3+}\text{AlSiO}_6$, $\text{NaM}^{3+}\text{Si}_2\text{O}_6$, and $\text{LiM}^{3+}\text{Si}_2\text{O}_6$. Note that within each series, $\langle\text{M}(2)\text{-O}\rangle$ distance increases with the increase of the $\langle\text{M}(1)\text{-O}\rangle$ distance, although the M(2) site is occupied by the same cation. To explore the interaction of the three types of polyhedra in the pyroxene structure, we need three dimensional plots of $\langle\text{M}(1)\text{-O}\rangle$, $\langle\text{M}(2)\text{-O}\rangle$ and the dimensions of the TO_4 tetrahedra, such as the $\langle\text{T-O}_{\text{br}}\rangle$, $\langle\text{T-O}_{\text{nbr}}\rangle$, the $\text{O}(3)\text{-O}(3')$ edge and the chain-kinking angle $\text{O}(3)\text{-O}(3')\text{-O}(3'')$ (Table 7). However, since $\langle\text{M}(2)\text{-O}\rangle$ is a linear function of $\langle\text{M}(1)\text{-O}\rangle$ (Fig. 2), we have taken the ratio $\langle\text{M}(1)\text{-O}\rangle/\langle\text{M}(2)\text{-O}\rangle$ as a measure of the interaction between the M(1) and M(2) polyhedra and plotted the dimensions of the TO_4 tetrahedra against this ratio in Figures 3 and 4. The average T-O_{br} bonds are the most flexible within the TO_4 tetrahedron and are strongly dependent on the ratio of the $\langle\text{M}(1)\text{-O}\rangle$ and $\langle\text{M}(2)\text{-O}\rangle$, distances whereas the average T-O_{nbr} bonds are quite rigid (Fig. 3). The relatively flexible tetrahedral edge, $\text{O}(3)\text{-O}(3')$, which is shared with the M(2) polyhedron (except Li) (Fig. 4a), and the tetrahedral-chain kinking angle, $\text{O}(3)\text{-O}(3')\text{-O}(3'')$, which matches the octahedral-chain repeat along the c axis, also depend on this effect (Fig. 4b) (cf. Cameron and Papike, 1980, 1981).

ACKNOWLEDGMENTS

We are indebted to A. Navrotsky, Princeton University, for her generosity in donating the samples. This research has been supported by the NASA Grant NGR 48-002-149 and (in part) NSF Grant EAR 82-06526.

REFERENCES

- Cameron, M., and Papike, J.J. (1980) Crystal chemistry of silicate pyroxenes. *Mineralogical Society of America Reviews of Mineralogy*, 7, 5-92.
- (1981) Structural and chemical variations in pyroxenes. *American Mineralogist*, 66, 1-50.
- Cameron, M., Sueno, S., Papike, J.J., and Prewitt, C.T. (1973) High temperature crystal chemistry of acmite, diopside, hedenbergite, jadeite, spodumene, and ureyite. *American Mineralogist*, 58, 594-618.
- Clark, J.R., Appleman, D.E., and Papike, J.J. (1969) Crystal chemical characterization of clinopyroxenes based on eight new structure refinements. *Mineralogical Society of America Special Paper* 2, 31-50.
- Cromer, D.T. (1965) Anomalous dispersion corrections computed from self-consistent field relativistic Dirac-Slater wave function. *Acta Crystallographica*, 18, 17-23.
- Cromer, D.T., and Waber, J.T. (1965) Scattering factors computed from relativistic Dirac-Slater wave functions. *Acta Crystallographica*, 18, 104-109.
- Finger, L.W. (1969) Determination of cation distributions by least-squares refinement of single crystal X-ray data. *Carnegie Institution of Washington Year Book* 67, 216-217.
- Freed, R.L., and Peacor, D.R. (1967) Refinement of the crystal structure of johannsenite. *American Mineralogist*, 52, 709-720.
- Ghose, S., and Wan, C. (1975) Crystal structures of $\text{CaCoSi}_2\text{O}_6$ and $\text{CaNiSi}_2\text{O}_6$: Crystal chemical relations in $C2/c$ pyroxenes (abs.). *EOS*, 56, 1076.
- Ghose, S., Okamura, F.P., and Ohashi, H. (1986) The crystal structure of $\text{CaFe}^{3+}\text{SiAlO}_6$ and crystal chemistry of $\text{Fe}^{3+}\text{-Al}^{3+}$ substitution in calcium Tschermak's pyroxene. *Contributions to Mineralogy and Petrology*, 92, 530-535.
- Ghose, S., McMullan, R.K., and Schomaker, V. (1987) Enstatite, $\text{Mg}_2\text{Si}_2\text{O}_6$: A neutron diffraction refinement of the crystal structure and a rigid-body analysis of the thermal vibration. *Zeitschrift für Kristallographie*, in press.
- Hawthorne, F.C., and Grundy, H.D. (1973) Refinement of the crystal structure of $\text{NaScSi}_2\text{O}_6$. *Acta Crystallographica*, B29, 2615-2616.
- (1974) Refinement of the crystal structure of $\text{NaInSi}_2\text{O}_6$. *Acta Crystallographica*, B30, 1882-1884.
- (1977) Refinement of the crystal structure of $\text{LiScSi}_2\text{O}_6$. *Canadian Mineralogist*, 15, 50-58.
- Levien, L., and Prewitt, C.T. (1981) High pressure structural study of diopside. *American Mineralogist*, 66, 315-323.
- Navrotsky, A., and Coons, W.E. (1976) Thermochemistry of some pyroxenes and related compounds. *Geochimica et Cosmochimica Acta*, 40, 1281-1288.
- Ohashi, H., and Ii, N. (1978) Structure of CaScAlSiO_6 -pyroxene. *Journal of the Japanese Association for Mineralogy, Petrology and Economic Geology*, 73, 267-273.
- Okamura, F.P., Ghose, S., and Ohashi, H. (1974) Structure and crystal chemistry of calcium Tschermak's pyroxene, CaAlAlSiO_6 . *American Mineralogist*, 59, 549-557.
- Ribbe, P.H., and Prunier, A.R., Jr. (1977) Stereochemical systematics of ordered $C2/c$ silicate pyroxenes. *American Mineralogist*, 62, 710-720.
- Schlenker, J.L. (1976) Phenomenological aspects of thermal expansion in crystals of the lower symmetry classes and the crystal structures of $\text{CaCoSi}_2\text{O}_6$ and $\text{CaNiSi}_2\text{O}_6$. Ph.D. thesis, Virginia Polytechnic Institute and State University, Blacksburg, Virginia.
- Shannon, R.D., and Prewitt, C.T. (1970) Revised values of effective ionic radii. *Acta Crystallographica*, B26, 1046-1048.

MANUSCRIPT RECEIVED FEBRUARY 24, 1986

MANUSCRIPT ACCEPTED NOVEMBER 7, 1986